

Circ_0000140 Alters miR-527/SLC7A11-Mediated Ferroptosis to Influence Oral Squamous Cell Carcinoma Cell Resistance to DDP

Yu Ma , Jinbo Gao, Hongning Guo

Department of Stomatology, Tianjin Third Central Hospital, Tianjin, People's Republic of China

Correspondence: Yu Ma, Department of Stomatology, Tianjin Third Central Hospital, No. 83 Jintang Road, Hedong District, Tianjin, 300170, People's Republic of China, Tel +86-13102229881, Email mayu881@tom.com

Background: While there is prior evidence for the ability of circular RNAs (circRNAs) to shape the cisplatin (DDP) resistance of cancers in human patients, there has been relatively little research to date focused on the interplay between circRNAs and DDP resistance in the context of OSCC progression to date. In the present analysis, the functional role that circ_0000140 plays as a mediator of chemoresistance to DDP was thus explored in greater detail.

Methods: Both qPCR and Western immunoblotting were employed as appropriate to detect circ_0000140, miR-527, and SLC7A11 levels, while interactions among these factors were detected through RNA immunoprecipitation, RNA pull-down, and dual luciferase report assays. MTT assays were used to assess cellular viability as a means of gauging DDP sensitivity.

Results: Both tissue samples from DDP-resistant OSCC patient tumors and OSCC cell lines resistant to DDP exhibited pronounced circ_0000140 upregulation. Knocking down this circRNA significantly increased the DDP sensitivity of both tested DDP-resistant OSCC cell lines and promoted ferroptosis, whereas knocking down miR-527 was sufficient to reverse these effects, which were recapitulated by miR-527 overexpression. Conversely, the effects of overexpressing miR-527 were reversed by the restoration of SLC7A11 expression. Consistently, this circRNA was able to increase DDP IC50 values and to suppress ferroptosis in both tested cell lines through this miR-527/SLC7A11 signaling axis.

Conclusion: These results revealed that circ_0000140/miR-527/SLC7A11-mediated ferroptosis may provide novel insights into the development of this cancer type and the emergence of chemoresistance in the future.

Keywords: Circ_0000140, DDP resistance, oral squamous cell carcinoma, miR-527, SLC7A11, ferroptosis

Introduction

As one of the most prevalent forms of head and neck squamous cell carcinoma (HNSCC),^{1,2} oral squamous cell carcinoma (OSCC) is generally treated through surgical, chemotherapeutic, and radiotherapeutic methods. While cisplatin (DDP) is a mainstay of the first-line chemotherapeutic treatment of many patients diagnosed with HNSCC,^{3,4} innate or acquired DDP resistance is a very common finding in OSCC patients,⁵ thereby complicating efforts to effectively treat this disease.⁶ OSCC patients face very high rates of morbidity and mortality, with 5-year survival rates that still remain relatively poor despite intensive research efforts focused on improving patient outcomes.^{2,7} As such, there is a pressing need to further explore the mechanistic drivers of DDP chemoresistance in patients with OSCC in an effort to reduce the devastating burden associated with this cancer type.

Circular RNAs (circRNAs) are transcripts that exhibit a closed-loop structure and that play diverse regulatory roles related to genomic imprinting, genome packaging, the regulation of target genes, and the modification of the chromatin.^{8,9} The dysregulation of these circRNAs has been shown to be significantly associated with oncogenic processes,¹⁰ and patterns of altered circRNA expression have even been reported in OSCC patient tumors.^{11,12} A growing wealth of evidence further supports an association between circRNAs and OSCC patient clinicopathological

characteristics^{13,14} or malignant OSCC cell growth.¹⁵ Several studies have also demonstrated that certain circRNAs are related to DDP resistance in a variety of human tumor types,^{16,17} including OSCC.^{6,18} Strikingly, high levels of the KIAA0907-derived circRNA circ_0000140 have previously been reported in OSCC,¹⁹ yet the mechanistic role that circ_0000140 plays in this malignant setting has yet to be established. The precise role of circ_0000140 remains largely undisclosed in OSCC.

Ferroptosis is related to abnormal intracellular iron, lipid metabolism, and amino acid activities.²⁰ Recent reports have identified a potential link between ferroptosis and chemotherapeutic resistance in multiple tumor types, with the maintenance of appropriate intracellular cysteine homeostasis being central to the inhibition of ferroptosis.²¹ The cystine/glutamate antiporter system component solute carrier family 7 member 11 (SLC7A11) is essential for the biosynthesis of glutathione (GSH) and the ability of cells to resist ferroptosis.²² The induction of ferroptosis in OSCC cells has also been suggested as a potential means of overcoming DDP resistance.⁵ Efforts to characterize circRNA signaling pathways and associated regulatory processes may thus offer further insight into the relationship between circRNAs and chemotherapeutic resistance.

Here, circ_0000140 upregulation was detected in both DDP-resistant OSCC tissue and cell samples. Moreover, this circRNA was found to contribute to the development of DDP resistance at least in part through the inhibition of ferroptosis via a mechanism linked to the modulation of the miR-527/SLC7A11 axis. Further research focused on this circ_0000140/miR-527/SLC7A11 axis may thus provide new insights into the mechanisms that drive OSCC development.

Materials and Methods

Tissue Samples

In total, primary OSCC tissue samples were obtained from 132 patients undergoing treatment at the Tianjin Third Central Hospital. The Research Scientific Ethics Committee of Tianjin Third Central Hospital approved this study. This study was conducted according to the Declaration of Helsinki. All patients provided written informed consent, and tissue samples were harvested during radical resection surgery. Patients were classified as being DDP-sensitive (n= 72) or DDP-resistant (n=60) based on their clinical records following DDP treatment for two cycles (40 mg/m²) administered at weeks 1 and 4. DDP-sensitive tumors were defined as those tumors in which a $\geq 30\%$ reduction was observed for the largest lesion, while DDP-resistant tumors were those without any significant change following treatment with DDP. After collection, tumors were stored at -80°C .

DDP-Resistant OSCC Cells

The SCC-15 and CAL-27 human OSCC cell lines were obtained from the BCRJ cell bank (Beijing, China), while the control human oral keratinocyte (HOK) cell line was obtained from the Cell Bank of Type Culture Collection of the Chinese Academy of Sciences (Shanghai, China). DDP-resistant OSCC cells were prepared by exposing these parental cell lines to DDP (cat. 2251; TOCRIS, Shanghai, China), gradually increasing the treatment dose from 1 μM to 8 μM , followed by prolonged cultivation for 2 months in the presence of DDP (4 μM), thus yielding the SCC-15/DDP and CAL-27/DDP cell lines. Cells were cultured with DMEM (R&D SYSTEMS, Shanghai, China) containing 10% FBS (R&D SYSTEMS) in a humidified 5% CO₂ incubator at 37°C. These DDP-resistant cells were cultured in DDP-free media for 2 days prior to experimental use.

qPCR

Total RNA and gDNA were respectively extracted from cells with a Total RNA Extraction Kit (R1200; Solarbio, Beijing, China) and a Universal Genomic DNA Extraction Kit (D2100; Solarbio). RNA samples were then used to prepare cDNA with a First Strand cDNA Synthesis Kit (K621; Thermo Fisher, MD, USA) or a miRNA First Strand cDNA Synthesis Kit (B532453; Songon). qPCR analyses were then conducted with 2X SYBR Green Abstart PCR Mix (B110031; Songon) and a miRNA qPCR Kit (B532461; Songon) to detect circ_0000140, miR-527, and SLC7A11, with U6 and GAPDH serving as normalization controls. The $2^{-\Delta\Delta\text{CT}}$ method was employed to assess relative gene expression.

MTT Assays

Parental or DDP-resistant CAL-27 and SCC-15 cells that were or were not transfected with treated with DDP for 48 h, after which media was replaced with media containing the MTT reagent (2 mg/mL). Following incubation for 4 h, media was removed from each well and replaced with 100 μ L of DMSO. Samples were shaken for 10 min, and absorbance at 490 nm was assessed via microplate reader. After constructing dose-response curves, DDP half-maximal inhibitory concentration (IC₅₀) values were calculated with GraphPad Prism 8.0 (GraphPad, CA, USA).

Luciferase Reporter Assays

Cells were added to 24-well plates (5×10^4 /well) followed by co-transfection with miR-527 mimics and WT or mutant (MUT) luciferase reporter plasmid constructs. Following incubation for 48 h, a luciferase reporter assay kit (Promega, USA, E1910) was used based on provided instructions. The pmirGLO plasmids were used to construct reporter plasmids containing WT and MUT circ_0000140 and SLC7A11 3'UTR reporter constructs.

RNA Immunoprecipitation (RIP)

RIP were performed according to the instructions of EZ-Magna RIP kit (Millipore). 1×10^7 cells were pelleted and resuspended with RIP lysis buffer plus protease and RNase inhibitors. The cell lysates were incubated with human anti-AGO2 antibody (Abcam) or mouse immunoglobulin G (IgG; Millipore) at 4°C overnight. The immunoprecipitated RNAs were extracted using the RNeasy MinElute Cleanup Kit (Qiagen, China) and reverse transcribed using the Goldenstar™ RT6 cDNA Synthesis Kit (TSINGKE). The abundance of circ_0000140, miR-527 and SLC7A11 was detected by qRT-PCR assay.

RNA Pull-Down Assay

Biotinylated circ_0000140 (Bio- circ_0000140) and control (Bio-NC) probes were added to M-280 streptavidin Dynabeads (Invitrogen) and allowed to incubate at 37°C for 2 h. Cell lysates were incubated for a further 3 h with the beads at 4°C. A qPCR approach was then employed to assess miR-527 expression.

Western Immunoblotting

Equal protein amounts were separated by SDS-PAGE, transferred to PVDF membranes (Bio-Rad, USA, 162–0177), and these blots were blocked with 5% skim milk before probing overnight with anti-SLC7A11 (Abcam, USA, ab37185) and anti- β -actin (Abcam, ab8227) at 4°C. After probing for 2 h using secondary antibodies at room temperature, proteins were detected with an ECL reagent (Sigma, USA, WBULS0100).

Statistical Analysis

Data are means \pm SD. Results were compared in GraphPad Prism 5.0 via Student's *t*-tests or ANOVAs. $P < 0.05$ served as the cut-off for statistical significance.

Results

DDP-Resistant OSCC Patient Tumors and Cell Lines Exhibit Circ_0000140

Upregulation

Relative to patients with DDP-sensitive OSCC, tumor tissues from individuals with DDP-resistant disease exhibited significantly increased circ_0000140 expression as detected via qPCR (Figure 1A). Consistently, this circRNA was expressed at higher levels in the SCC-15 and CAL-27 tumor cell lines relative to control HOK cells, and it was further upregulated in the SCC-15/DDP and CAL-27/DDP cells as compared to corresponding parental controls (Figure 1B). In contrast to levels of linear KIAA0907, RNaseR treatment largely failed to impact circ_0000140 levels in SCC-15/DDP or CAL-27/DDP cells (Figure 1C and D). The expression of circ_0000140 was largely observed in the cytosol, with a localization pattern consistent with that of GAPDH and distinct from that of U6 (Figure 1E and F). This suggests that stable circ_0000140 upregulation occurs in OSCC, particularly in the context of chemoresistant to DDP.

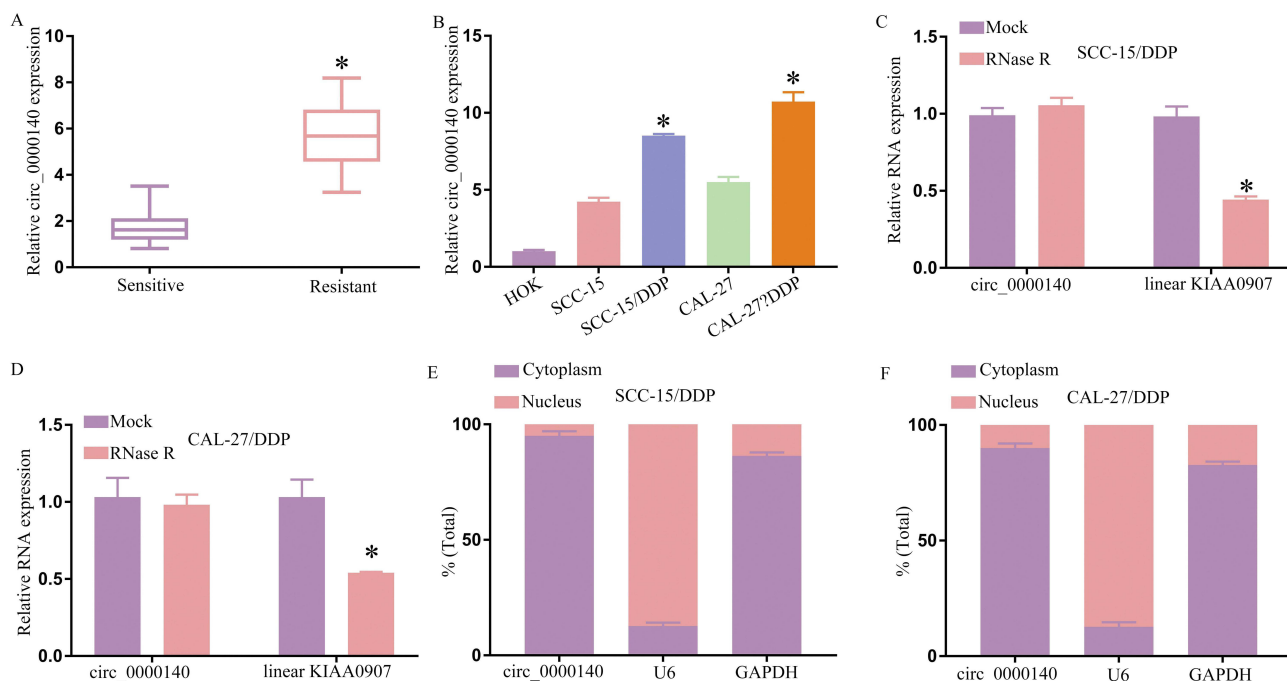


Figure 1 OSCC cells and tissues resistant to DDP exhibit circ_0000140 upregulation. A qPCR approach was employed to detect the expression of circ_0000140 in samples of DDP-sensitive or –resistant tumor tissue samples (A) or in parental or DDP-resistant OSCC tumor cell lines, with HOK cells serving as normal controls (B). (C and D). qPCR was used to detect linear KIAA0907 and circ_0000140 expression following control or RNase R treatment. (E and F). Levels of cytosolic and nuclear circ_0000140 and U6 were detected, with GAPDH having been analyzed to normalize these results. Results are means \pm SD, *P < 0.05.

Silencing Circ_0000140 Overcomes OSCC Cell Resistance to DDP Treatment via the Inhibition of Ferroptosis

After establishing the DDP-resistant SCC-15/DDP and CAL-27/DDP cell lines, an MTT assay was performed which revealed that while both these cells and their corresponding parental lines were less viable following DDP treatment (Figure 2A), the DDP IC₅₀ values for these SCC-15/DDP and CAL-27/DDP cells were substantially increased (Figure 2B). These findings thus confirmed that these cells had acquired a DDP-resistant phenotype. When an siRNA approach was used to knock down circ_0000140 in these cells, this circRNA was markedly downregulated in both of these DDP-resistant OSCC cell lines (Figure 2C). Significantly lower DDP IC₅₀ values were also observed in these DDP-resistant OSCC cells following the knockdown of circ_0000140 (Figure 2D). This circ_0000140 silencing also contributed to increases in ferroptosis-related biomarkers including Fe²⁺, iron, and ROS levels in these SCC-15/DDP and CAL-27/DDP cells (Figure 2E–G), with erastin having been utilized as a positive control to induce ferroptosis. As such, these findings highlight the ability of circ_0000140 to induce chemoresistance in OSCC cells at least in part via the inhibition of ferroptosis.

Circ_0000140 Serves as a Molecular Sponge in OSCC Cells Capable of Sequestering miR-527

Subsequent experiments revealed that circ_0000140 can influence chemoresistance within OSCC cells by serving as a molecular sponge to sequester target miRNAs. The starBase v2.0 algorithm identified complementary binding sequences suggesting that miR-527 can interact with circ_0000140 (Figure 3A). This binding interaction was confirmed through a dual-luciferase reporter assay in which the co-transfection of DDP-resistant OSCC cell lines with miR-527 mimic constructs and a WT-circ_0000140 vector resulted in a drop in luciferase activity that was not evident if a MUT-circ_0000140 construct was instead used (Figure 3B and C). In a RIP assay system, precipitation mediated by Argonaute2 (Ago2) also led to the concurrent enrichment of circ_0000140 and miR-527 from these cells (Figure 3D and E), while the use of bio-miR-527 for an RNA pull-down assay also led to circ_0000140 enrichment in the resultant

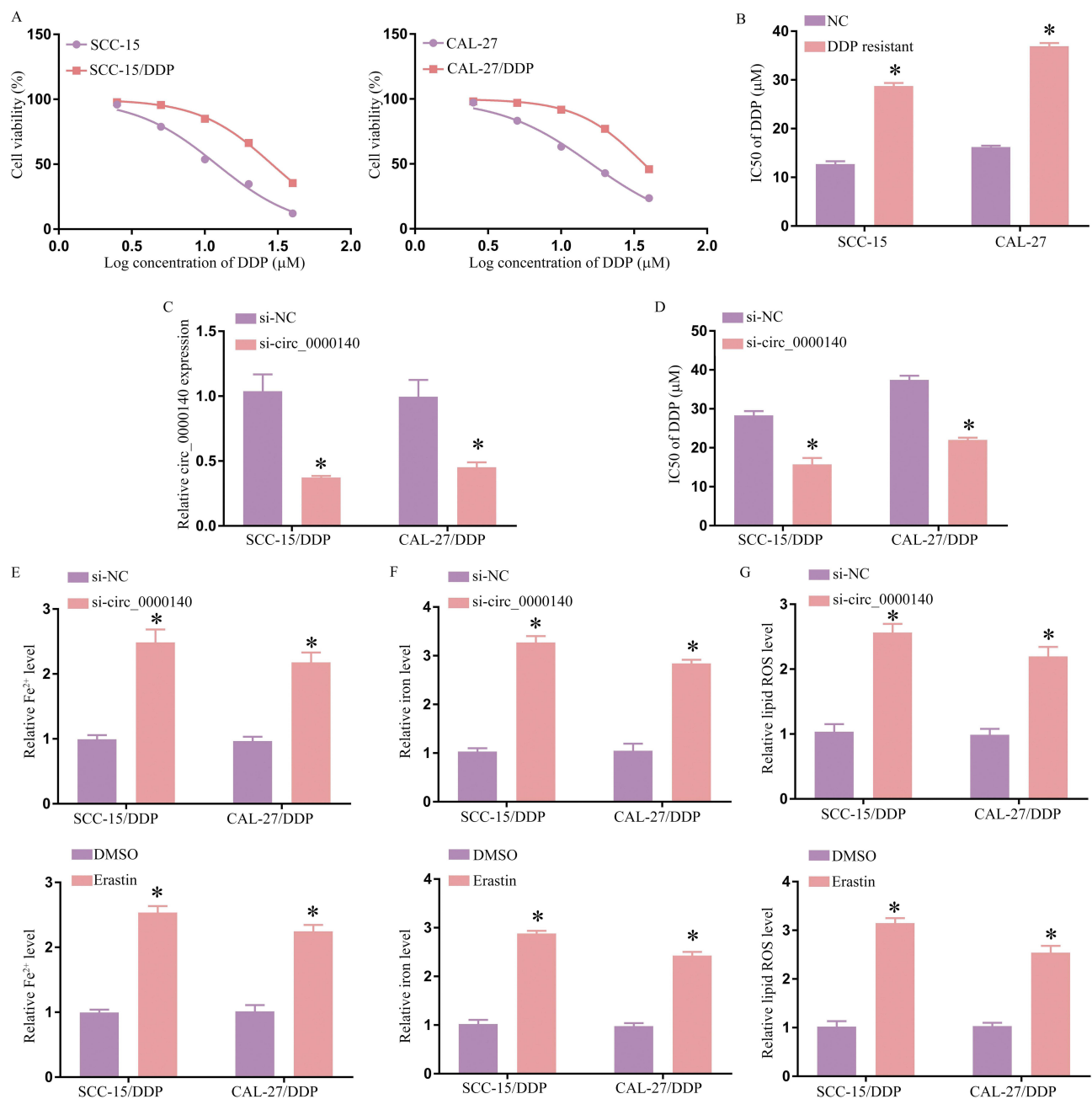


Figure 2 Knocking down circ_0000140 suppresses OSCC cell chemoresistant phenotypes through the inhibition of ferroptosis. (A) The viability of parental and DDP-resistant SCC-15 and CAL-27 cells was analyzed via MTT assay. (B) Dose-response curves were used to compute DDP IC50 values for the indicated cell lines. (C) The expression of circ_0000140 was analyzed via qPCR. (D) DDP IC50 values were established through an MTT assay. (E–G) Iron, Fe²⁺, and ROS levels in DDP-resistant OSCC cell lines were measured. Results are means ± SD, *P < 0.05.

precipitate (Figure 3F and G). Lower levels of miR-527 expression were detectable in tumor tissue samples from OSCC patients with DDP-resistant disease and in SCC-15/DDP and CAL-27/DDP cells relative to corresponding control samples and cells sensitive to DDP (Figure 3H and I). The expression of miR-527 was also negatively correlated with circ_0000140 levels in OSCC patients with DDP-resistant disease (Figure 3J), and qPCR analyses confirmed that miR-527 expression was further suppressed by overexpressing circ_0000140 in both tested DDP-resistant OSCC cell lines (Figure 3K and L). Conversely, the siRNA-mediated knockdown of circ_0000140 resulted in an increase in miR-527 expression (Figure 3L). These data thus revealed that circ_0000140 can serve as a molecular sponge that suppresses miR-527 expression in OSCC.

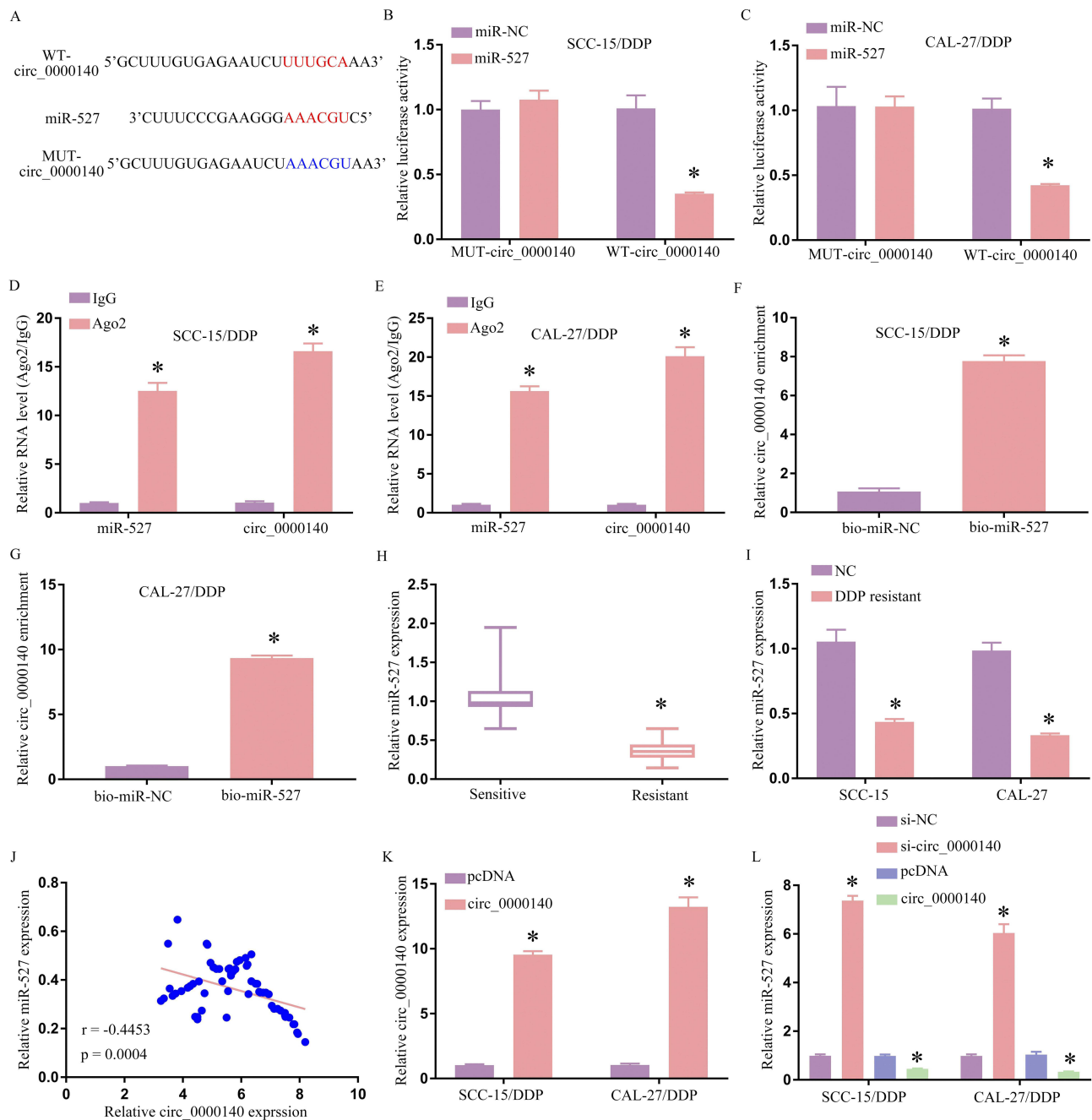


Figure 3 Circ_0000140 serves as a molecular sponge that can sequester miR-527 within OSCC cells. **(A)** Complementary sequence overlap was detected between miR-527 and wild-type (WT) circ_0000140, with corresponding mutant (MUT) circRNA sequences also being shown. **(B and C)** Following the co-transfection of DDP-resistant OSCC cells with both the WT- or MUT-circ_0000140 reporter constructs and either miR-527 or miR-NC, these cells were analyzed in a dual-luciferase assay. **(D and E)** Extracts prepared from the indicated DDP-resistant cell lines were used for RIP assays in which miR-527 and circ_0000140 levels were detected following Ago2 or control IgG immunoprecipitation. **(F and G)** The enrichment of circ_0000140 was assessed in extracts prepared from the indicated DDP-resistant cells following biotinylated (bio)-miR-527 or bio-miR-NC transfection in an RNA pull-down assay. **(H–I)** The expression of miR-527 was assessed via qPCR in OSCC tissue samples from the indicated resistant or sensitive patients. **(J)** Pearson's correlation analyses (r) were used to explore the association between the expression of circ_0000140 and miR-527 in tissue samples from resistant OSCC patients. **(K)** The levels of circ_0000140 were assessed in SCC-15/DDP and CAL-27/DDP cells following transfection with a vector to overexpress circ_0000140 or a control pcDNA vector. **(L)** The expression of miR-527 was assessed in the indicated DDP-resistant OSCC cells following si-NC, si-circ_0000140, pcDNA, or circ_0000140 transfection. Results are means \pm SD, * $P < 0.05$.

The Knockdown of Circ_0000140 Liberates miR-527 and Restores Chemosensitivity in DDP-Resistant OSCC Cells

The SCC-15/DDP and CAL-27/DDP cells were next transfected with si-circ_0000140 with or without anti-miR-527 to conduct a series of rescue experiments, with qPCR being used to confirm that anti-miR-527 successfully abrogated the

circ_0000140 knockdown-associated upregulation of this miRNA (Figure 4A). The reduction in DDP IC50 values observed following the knockdown of circ_0000140 was also reversed by anti-miR-527 in both tested DDP-resistant cell lines (Figure 4B). Circ_0000140 silencing led to increases in ferroptosis-related iron, Fe²⁺, and ROS levels that were also reversed by anti-miR-527 in these two OSCC cell lines (Figure 4C–E). Together, these data provide evidence demonstrating that the loss of circ_0000140 may contribute to miR-527 upregulation, thereby overcoming DDP resistance in OSCC cells, whereas the downregulation of miR-527 was sufficient to reverse this effect.

miR-527 Targets and Suppresses the Expression of SLC7A11

Next, the starBase v2.0 algorithm was leveraged in an effort to identify candidate targets of miR-527, revealing a complementary binding site present within the 3'-UTR of SLC7A11 (Figure 5A). Following miR-527 mimic co-transfection, reductions in WT-SLC7A11-3'UTR reporter vector luciferase activity was evident in both tested DDP-resistant OSCC cell lines (Figure 5B and 5C). A RIP assay also revealed clear concurrent miR-527 and SLC7A11 enrichment following Ago2 precipitation (Figure 5D and E), while RNA pull-down analyses demonstrated that SLC7A11 was enriched following the use of bio-miR338-3p to mediate precipitation (Figure 5F and G). OSCC tissue samples from DDP-resistant patients exhibited markedly increased protein and mRNA levels (Figure 5H and I), and both SCC-15 and CAL-27 cells also exhibited higher SLC7A11 protein levels as compared to HOK control cells, while this protein was further upregulated in the SCC-15/DDP and CAL-27/DDP cell lines (Figure 5J). Moreover, miR-527 and SLC7A11 levels were negatively correlated in OSCC patient tumor tissues from individuals resistant to DDP (Figure 5K). Together, these findings thus support the ability of miR-527 and SLC7A11 to directly interact within OSCC cells. Consistently, Western immunoblotting revealed that the knockdown of circ_0000140 was associated with a drop in the expression of SLC7A11 in both DDP-resistant cell lines, while this was rescued by anti-miR-527 treatment (Figure 6L). As such, these results suggest that the circ_0000140/miR-527/SLC7A11 pathway serves as a modulator of chemoresistance of DDP in OSCC.

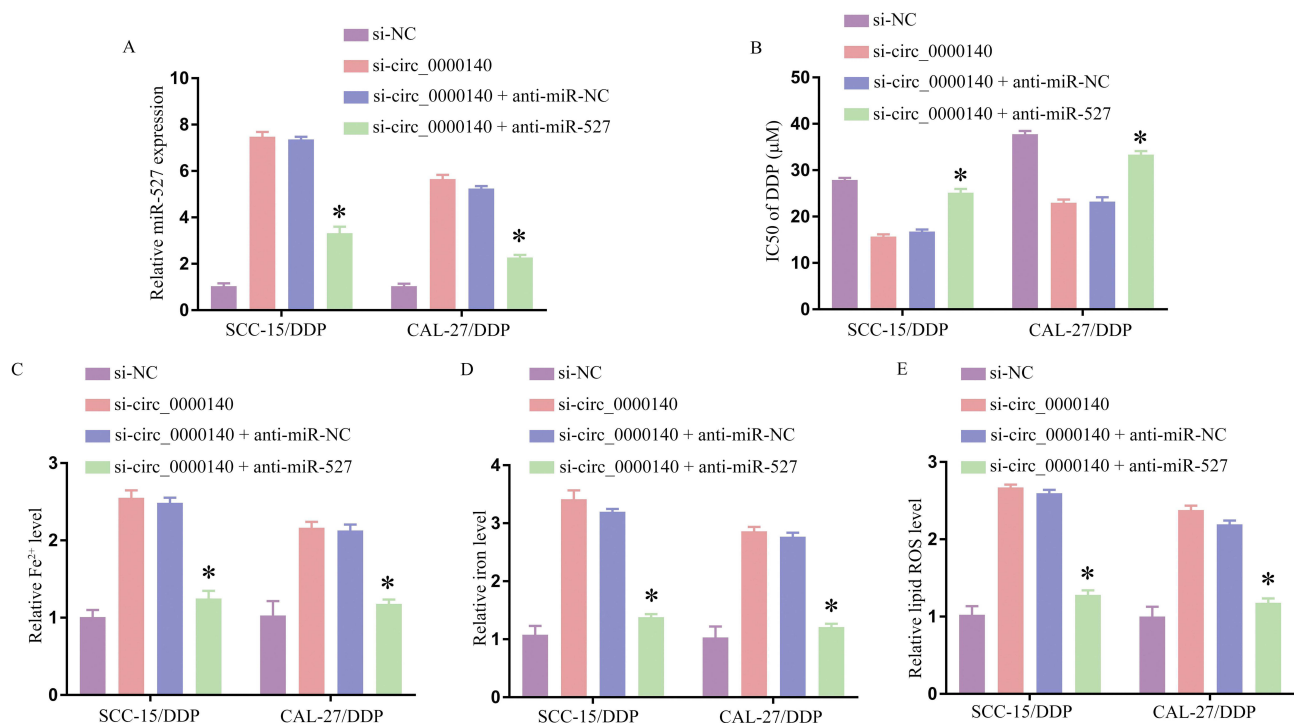


Figure 4 Reductions in circ_0000140 expression liberate miR-527 and thereby suppress chemoresistant properties in DDP-resistant OSCC cell lines. (A) miR-527 expression was detected via qPCR following transfection, with U6 as a normalization control. (B) DDP IC50 values were detected following transfection through an MTT assay approach. C–E. Iron, Fe²⁺, and ROS levels were detected after transfection in the indicated DDP-resistant cell lines. Results are means ± SD, *P < 0.05.

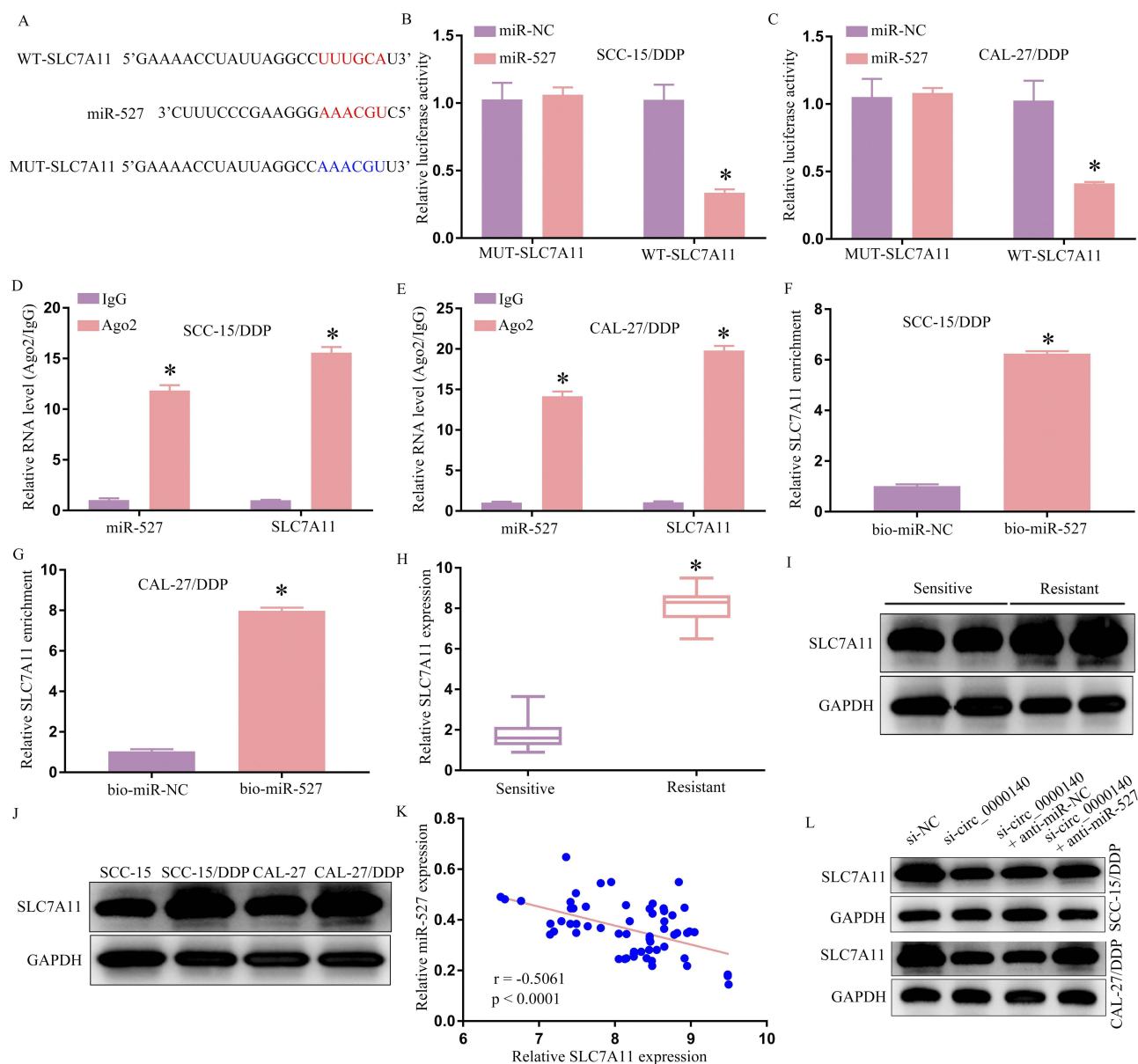


Figure 5 miR-527 targets SLC7A11. **(A)** Complementary miR-527 and SLC7A11 3'-UTR sequences were detected using the starBase v2.0 algorithm, with both WT and MUT versions of this 3'-UTR sequence being shown. **(B and C)** Following the co-transfection of DDP-resistant OSCC cells with both the WT- or MUT-SLC7A11 3'-UTR reporter constructs and either miR-527 or miR-NC, these cells were analyzed in a dual-luciferase assay. **(D and E)** Extracts prepared from the indicated DDP-resistant cell lines were used for RIP assays in which miR-527 and SLC7A11 levels were detected following Ago2 or control IgG immunoprecipitation. **(F and G)** The enrichment of SLC7A11 was assessed in extracts prepared from the indicated DDP-resistant cells following bio-miR-527 or bio-miR-NC transfection in an RNA pull-down assay. **(H-J)** SLC7A11 mRNA **(H)** and protein **(I-J)** levels were detected in resistant or sensitive OSCC patient tissue samples and the indicated control, parental, or DDP-resistant cells. **(K)** Pearson's correlation analyses (r) were used to explore the association between the expression of SLC7A11 and miR-527 in tissue samples from resistant OSCC patients. **(L)** SLC7A11 protein levels were detected via Western immunoblotting following transfection in the CAL-27/DDP and SCC-15/DDP cell lines. GAPDH served as a normalization control for all Western immunoblotting. Results are means \pm SD, * $P < 0.05$.

Overexpressing miR-527 Suppresses DDP Resistance in OSCC Cells Through the Downregulation of SLC7A11

In a final series of experiments, the relationship between OSCC cell DDP resistance and both miR-527 and SLC7A11 expression was explored. Functional assays were performed following the transfection of DDP-resistant cells with a miR-527 mimic with or without a vector to induce SLC7A11 overexpression. SLC7A11 protein levels were notably reduced in both SCC-15/DDP and CAL-27/DDP cells following transfection with this miRNA mimic, while overexpressing SLC7A11 effectively reversed this downregulation (Figure 6A). This miR-527 mimic suppressed the IC₅₀ values for

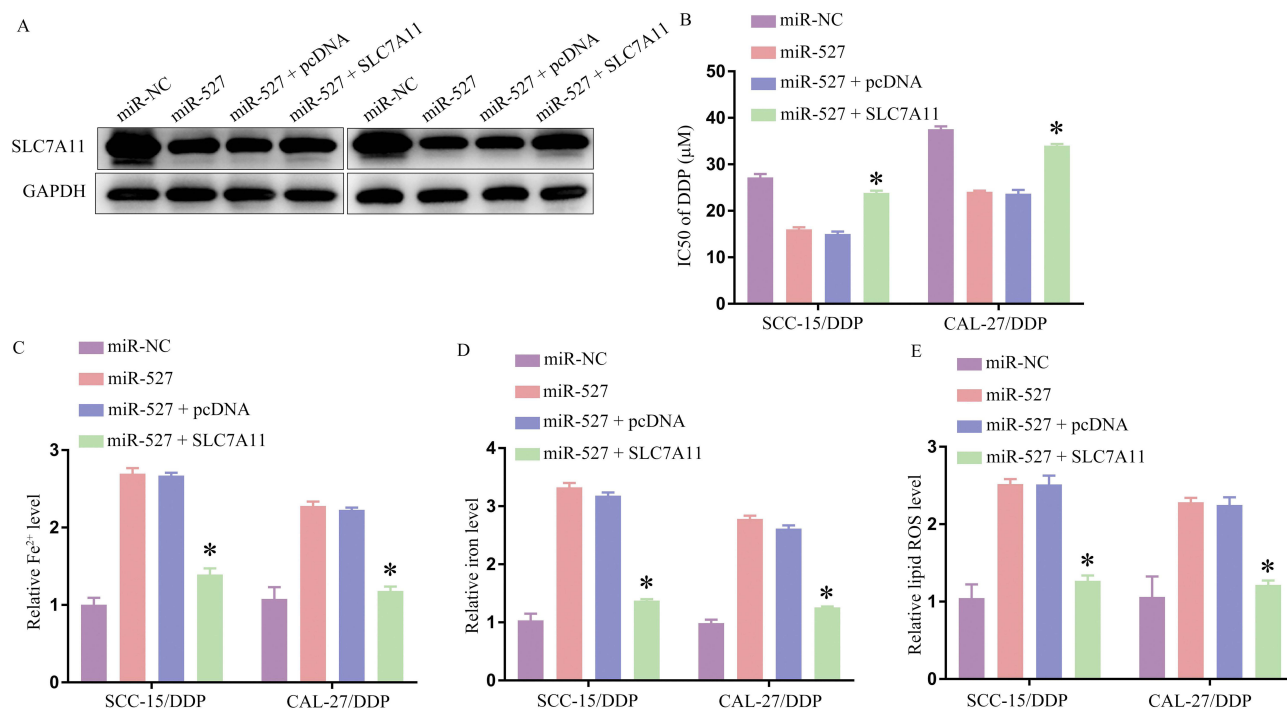


Figure 6 Overexpressing miR-527 downregulates SLC7A11 to overcome DDP resistance in OSCC cell lines. (A). SLC7A11 protein levels were detected via Western immunoblotting following transfection. (B). DDP IC₅₀ values in the indicated cell lines were calculated following transfection. (C–E). Iron, Fe²⁺, and ROS levels were detected in transfected DDP-resistant cell lines. Results are means ± SD, *P < 0.05.

DDP in both tested cell lines (Figure 6B), and corresponding increases in ferroptotic markers including Fe²⁺, iron, and ROS production were also observed in these transfected cells (Figure 6C–E). This is consistent with the ability of miR-527 to overcome resistance to DDP through the regulation of SLC7A11 expression.

Discussion

DDP is often used as a first-line choice when treating patients with OSCC, as this chemotherapeutic drug can effectively kill target tumor cells.¹⁸ Many studies have shown that circRNAs can serve as dynamic regulators of key chemoresistance and chemosensitization mechanisms in a variety of cancer types.^{23,24} Given that ferroptosis has been recognized as an important factor related to cancer treatment, this study sought to explore the mechanisms through which circ_0000140 modulates ferroptosis to influence chemoresistance in OSCC. Both OSCC patient tissues and DDP-resistant cell lines exhibited elevated levels of circ_0000140 expression, and knocking down this circRNA contributed to increases in ferroptotic activity with a corresponding drop in cellular viability. This suggests that circ_0000140 may play a previously unrecognized oncogenic role in OSCC in addition to promoting chemoresistance, and further research is warranted to expand these analyzed to other malignant tumor types.

The best-characterized mechanisms through which circRNAs function relate to their ability to sequester specific miRNAs, thus interfering with their functionality. Accordingly, a bioinformatics approach was employed to screen for possible target miRNAs associated with circ_0000140, ultimately confirming the identification of miR-527 as one such target. Further research confirmed that in OSCC cells, circ_0000140 was able to promote SLC7A11 upregulation through its ability to function as a molecular sponge for miR-527, an miRNA that has not previously been characterized in the context of OSCC. Notably, miR-527 downregulation was detected in tissue samples from DDP-resistant OSCC patients, and it was found to shape chemoresistance in OSCC cells at least in part via a circRNA-miRNA interaction mechanism. There is prior evidence supporting the link between miR-527 and chemoresistance in a range of cancer types. For example, circ_C20orf11 enhances DDP resistance by inhibiting miR-527/YWHAZ through the promotion of extracellular vesicle-mediated macrophage M2 polarization in ovarian cancer.²⁴ The present data indicate that miR-527 shapes

DDP resistance in OSCC cells at least in part by modulating the expression of SLC7A11. By directly binding to miR-527, circ_0000140 is able to suppress its regulatory function, thus indicating that circ_0000140 may contribute to the development of DDP-resistant OSCC through the sequestration of miR-527.

The inhibition of SLC7A11 can induce ferroptosis, thereby overcoming therapeutic resistance in tumor cells.²⁵ In ovarian cancer, erastin has been demonstrated to overcome ABCB1-mediated docetaxel resistance and to promote ferroptosis,²⁶ which is particularly notable given that this drug is the most potent SLC7A11 inhibitor identified to date, providing a mechanistic basis for this chemosensitizing activity. The present data support these prior results, confirming the potential therapeutic viability of SLC7A11 as a pharmacological target. The mechanisms that govern the development, progression, and chemoresistance of OSCC remain to be fully documented. These results offer novel evidence in support of the ability of DDP administration to induce ferroptosis in exposed OSCC cells, with the ability to resist ferroptotic activity thus contributing to overall tumor cell chemoresistance. Inhibiting circ_0000140 was also found to modulate the regulation of SLC7A11 and ferroptosis. At the molecular level, the inhibition of this circRNA was demonstrated to liberate miR-527, which in turn suppressed the expression of SLC7A11 whereas silencing miR-527 was sufficient to overcome this circ_0000140 inhibition-induced downregulation of SLC7A11. These data thus demonstrate that circ_0000140 modulates the miR-527/SLC7A11 axis to alter ferroptosis and chemoresistance in OSCC cells.

Conclusion

In summary, these findings offer a robust foundation for efforts to understand the emergence of DDP resistance in OSCC. Specifically, circ_0000140 was found for the first time to increase OSCC cell sensitivity to DDP treatment and ferroptosis through interactions with the miR-527 /SLC7A11 pathway. More broadly, this provides support for the therapeutic relevance of circRNAs in this oncologic setting and suggests that efforts to target this circ_0000140/miR-527/SLC7A11 axis may be a viable means of overcoming chemoresistance in OSCC patients undergoing clinical treatment.

Disclosure

The authors declare that they have no competing interests in this work.

References

1. Siegel RL, Miller KD, Wagle NS, Jemal A. Cancer statistics, 2023. *CA Cancer J Clin.* 2023;73(1):17–48. doi:10.3322/caac.21763
2. Almagush A, Makitie AA, Triantafyllou A, et al. Staging and grading of oral squamous cell carcinoma: an update. *Oral Oncol.* 2020;107:104799. doi:10.1016/j.oraloncology.2020.104799
3. Loeffler TM, Lindemann J, Luckhaupt H, Rose KG, Hausamen TU. Chemotherapy of advanced and relapsed squamous cell cancer of the head and neck with split-dose cisplatin (DDP), 5-fluorouracil (Fura) and leucovorin (CF). *Adv Exp Med Biol.* 1988;244:267–273.
4. Guigay J, Auperin A, Fayette J, et al. Cetuximab, docetaxel, and cisplatin versus platinum, fluorouracil, and cetuximab as first-line treatment in patients with recurrent or metastatic head and neck squamous-cell carcinoma (GORTEC 2014-01 TPEXtreme): a multicentre, open-label, randomised, Phase 2 trial. *Lancet Oncol.* 2021;22(4):463–475. doi:10.1016/S1470-2045(20)30755-5
5. Han L, Li L, Wu G. Induction of ferroptosis by carnosic acid-mediated inactivation of Nrf2/HO-1 potentiates cisplatin responsiveness in OSCC cells. *Mol Cell Probes.* 2022;64:101821. doi:10.1016/j.mcp.2022.101821
6. Gao F, Han J, Wang Y, Jia L, Luo W, Zeng Y. Circ_0109291 promotes cisplatin resistance of oral squamous cell carcinoma by sponging miR-188-3p to increase ABCB1 expression. *Cancer Biother Radiopharm.* 2022;37(4):233–245. doi:10.1089/cbr.2020.3928
7. Matsuura D, Valim TD, Kulcsar MAV, et al. Risk factors for salvage surgery failure in oral cavity squamous cell carcinoma. *Laryngoscope.* 2018;128(5):1113–1119. doi:10.1002/lary.26935
8. Kristensen LS, Andersen MS, Stagsted LVW, Ebbesen KK, Hansen TB, Kjems J. The biogenesis, biology and characterization of circular RNAs. *Nat Rev Genet.* 2019;20(11):675–691. doi:10.1038/s41576-019-0158-7
9. Chen LL. The expanding regulatory mechanisms and cellular functions of circular RNAs. *Nat Rev Mol Cell Biol.* 2020;21(8):475–490. doi:10.1038/s41580-020-0243-y
10. Lei M, Zheng G, Ning Q, Zheng J, Dong D. Translation and functional roles of circular RNAs in human cancer. *Mol Cancer.* 2020;19(1):30. doi:10.1186/s12943-020-1135-7
11. Paramasivam A. Circulating circular RNAs: novel potential biomarkers and therapeutic targets for oral cancer. *Oral Oncol.* 2022;134:106067. doi:10.1016/j.oraloncology.2022.106067
12. Peng QS, Cheng YN, Zhang WB, Fan H, Mao QH, Xu P. circRNA_0000140 suppresses oral squamous cell carcinoma growth and metastasis by targeting miR-31 to inhibit Hippo signaling pathway. *Cell Death Dis.* 2020;11(2):112. doi:10.1038/s41419-020-2273-y
13. Zhang L, Wang M, Ren W, et al. Prognostic significance of CircRNAs expression in oral squamous cell carcinoma. *Oral Dis.* 2023;29(4):1439–1453. doi:10.1111/odi.14188
14. Huang L, Pei T, Wu G, Liu J, Pan W, Pan X. Circular RNAs as a diagnostic biomarker in oral squamous cell carcinoma: a meta-analysis. *J Oral Maxillofac Surg.* 2022;80(4):756–766. doi:10.1016/j.joms.2021.11.021

15. Liu J, Jiang X, Zou A, et al. circIGHG-induced epithelial-to-mesenchymal transition promotes oral squamous cell carcinoma progression via miR-142-5p/IGF2BP3 signaling. *Cancer Res.* 2021;81(2):344–355. doi:10.1158/0008-5472.CAN-20-0554
16. Peng L, Sang H, Wei S, et al. circCUL2 regulates gastric cancer malignant transformation and cisplatin resistance by modulating autophagy activation via miR-142-3p/ROCK2. *Mol Cancer.* 2020;19(1):156. doi:10.1186/s12943-020-01270-x
17. Cao Y, Xie X, Li M, Gao Y. CircHIPK2 Contributes to DDP resistance and malignant behaviors of DDP-resistant ovarian cancer cells both in vitro and in vivo through circHIPK2/miR-338-3p/CHTOP ceRNA pathway. *Onco Targets Ther.* 2021;14:3151–3165. doi:10.2147/OTT.S291823
18. Qiu F, Qiao B, Zhang N, et al. Blocking circ-SCMH1 (hsa_circ_0011946) suppresses acquired DDP resistance of oral squamous cell carcinoma (OSCC) cells both in vitro and in vivo by sponging miR-338-3p and regulating LIN28B. *Cancer Cell Int.* 2021;21(1):412. doi:10.1186/s12935-021-02110-8
19. Guo J, Su Y, Zhang M. Circ_0000140 restrains the proliferation, metastasis and glycolysis metabolism of oral squamous cell carcinoma through upregulating CDC73 via sponging miR-182-5p. *Cancer Cell Int.* 2020;20:407. doi:10.1186/s12935-020-01501-7
20. Conrad M, Pratt DA. The chemical basis of ferroptosis. *Nat Chem Biol.* 2019;15(12):1137–1147. doi:10.1038/s41589-019-0408-1
21. Hadian K, Stockwell BR. A roadmap to creating ferroptosis-based medicines. *Nat Chem Biol.* 2021;17(11):1113–1116. doi:10.1038/s41589-021-00853-z
22. Chen X, Li J, Kang R, Klionsky DJ, Tang D. Ferroptosis: machinery and regulation. *Autophagy.* 2021;17(9):2054–2081. doi:10.1080/15548627.2020.1810918
23. Xie H, Yao J, Wang Y, Ni B. Exosome-transmitted circVMP1 facilitates the progression and cisplatin resistance of non-small cell lung cancer by targeting miR-524-5p-METTL3/SOX2 axis. *Drug Deliv.* 2022;29(1):1257–1271. doi:10.1080/10717544.2022.2057617
24. Yin J, Huang HY, Long Y, et al. circ_C20orf11 enhances DDP resistance by inhibiting miR-527/YWHAZ through the promotion of extracellular vesicle-mediated macrophage M2 polarization in ovarian cancer. *Cancer Biol Ther.* 2021;22(7–9):440–454. doi:10.1080/15384047.2021.1959792
25. Hong T, Lei G, Chen X, et al. PARP inhibition promotes ferroptosis via repressing SLC7A11 and synergizes with ferroptosis inducers in BRCA-proficient ovarian cancer. *Redox Biol.* 2021;42:101928. doi:10.1016/j.redox.2021.101928
26. Zhou HH, Chen X, Cai LY, et al. Erastin reverses ABCB1-mediated docetaxel resistance in ovarian cancer. *Front Oncol.* 2019;9:1398. doi:10.3389/fonc.2019.01398

Pharmacogenomics and Personalized Medicine

Dovepress

Publish your work in this journal

Pharmacogenomics and Personalized Medicine is an international, peer-reviewed, open access journal characterizing the influence of genotype on pharmacology leading to the development of personalized treatment programs and individualized drug selection for improved safety, efficacy and sustainability. This journal is indexed on the American Chemical Society's Chemical Abstracts Service (CAS). The manuscript management system is completely online and includes a very quick and fair peer-review system, which is all easy to use. Visit <http://www.dovepress.com/testimonials.php> to read real quotes from published authors.

Submit your manuscript here: <https://www.dovepress.com/pharmacogenomics-and-personalized-medicine-journal>